The top quark chromomagnetic dipole moment in the SM from the four-body vertex function

arXiv:2110.14125 [hep-ph]

Javier Montaño Domínguez
Investigadoras e Investigadores por México Conacyt
FCFM-UMSNH
en colaboración con
Fernando Iguazú Ramírez Zavaleta,
Eduardo Salvador Tututi Hernández,
Everardo Urquiza Trejo

XVIII MWPF

25/Nov/2022

Abstract

Based on the 5-dimension effective Lagrangian operator that characterizes the chromodipolar vertices $g\bar{t}t$ and $gg\bar{t}t$, the chromomagnetic dipole $\hat{\mu}_t$ is derived via quantum fluctuation at the 1-loop level from the $gg\bar{t}t$ vertex. We evaluate $\hat{\mu}_t(s)$ as a function of the energy scale $s = \pm E^2$, for $E = [10, 1000]$ GeV. At the typical energy scale $E = m_Z$, similarly to $\alpha_s(m_Z^2)$ for high-energy physics, the spacelike evaluation yields $\hat{\mu}_t(-m_Z^2) = -0.025+0.00384i$ and the timelike $\hat{\mu}_t(m_Z^2) = -0.0318-0.0106i$. This $\mathrm{Re}\,\hat{\mu}_t(-m_Z^2) = -0.025$ from $gg\bar{t}t$ is even closer to the experimental central value $\hat{\mu}_t^{\mathrm{Exp}} = -0.024$, than that coming from the known vertex $g\bar{t}t$, -0.0224. The $\mathrm{Im}\,\hat{\mu}_t(-m_Z^2)$ part is due to virtual charged currents. The spacelike prediction is the favored one, $\|\hat{\mu}_t^{\mathrm{3b}}(-m_Z^2)\| \lessapprox \|\hat{\mu}_t^{\mathrm{EXP}}\| \lessapprox \|\hat{\mu}_t^{\mathrm{4b}}(-m_Z^2)\|$.

1) The first dipolar interaction

- 1948. Schwinger published the anomalous magnetic dipole moment (AMDM) of the electron with the photon on-shell, $q^2 = 0$: $a_e = \alpha/2\pi$.

$$\mathcal{L}_{\text{eff}}^{5D} = -\frac{1}{2}\bar{f}_i\sigma^{\mu\nu}\left[F_M(q^2) + iF_E(q^2)\gamma_5\right] f_i F_{\mu\nu},$$

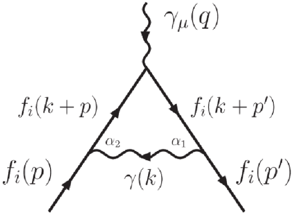

$$F_{\mu\nu} = \partial_\mu A_\nu - \partial_\nu A_\mu,$$

$$F_M(0) = \frac{eQ_{f_i}a_{f_i}}{2m_{f_i}},$$

$$F_E(0) = Q_{f_i}d_{f_i},$$

a_{f_i} is the AMDM and d_{f_i} is the electric dipole moment (EDM).

- The QED AMDM concept trivially extrapolates to Quantum Chromodynamics (QCD).

2) Anomalous chromoelectromagnetic dipole moment

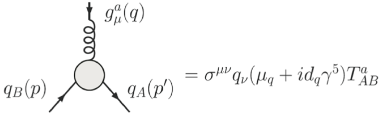

The effective Lagrangian characterizes the quantum loop induced chromoelectromagnetic dipole moments

$$\mathcal{L}^{5D}_{eff} = -\frac{1}{2} \bar{q}_A \sigma^{\mu\nu} \left[\mu_q(q^2) + i d_q(q^2) \gamma^5 \right] q_B G^a_{\mu\nu} T^a_{AB}, \qquad (1)$$

$$G^a_{\mu\nu} = \partial_\mu g^a_\nu - \partial_\nu g^a_\mu - g_s f_{abc} g^b_\mu g^c_\nu, \qquad (2)$$

T^a_{AB} is the $SU(3)_C$ color generator, and $\sigma^{\mu\nu} \equiv \frac{i}{2}[\gamma^\mu, \gamma^\nu]$. The dimensionless dipoles are

$$\hat{\mu}_q \equiv \frac{m_q}{g_s} \mu_q, \quad \hat{d}_q \equiv \frac{m_q}{g_s} d_q, \qquad (3)$$

the ACMDM $\hat{\mu}_q$ conserves CP, and the CEDM $\hat{d}_q$ violates CP, m_q is the quark mass, $g_s = \sqrt{4\pi\alpha_s}$ is the coupling constant of QCD with $\alpha_s(m_Z^2) = 0.1179$ characterized perturbatively at the energy scale m_Z for high-energy physics. In general $\hat{\mu}_q$ y $\hat{d}_q \in \mathbb{C}$, they may have absorptive imaginary parts. $q^2 = (p' - p)^2$.

3) Quantum fluctuation at the one-loop level in the SM

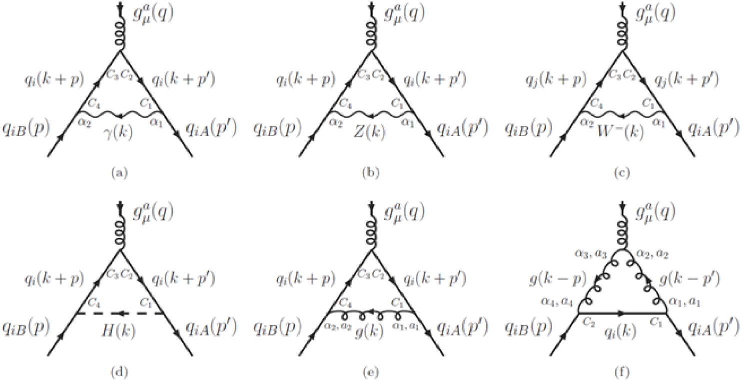

SM contribution to the ACMDM in the unitary Gauge, same result in the general R_ξ gauge:

$$\hat{\mu}_{q_i}(q^2) = \hat{\mu}_{q_i}(\gamma) + \hat{\mu}_{q_i}(Z) + \hat{\mu}_{q_i}(W) + \hat{\mu}_{q_i}(H) + \hat{\mu}_{q_i}(g) + \hat{\mu}_{q_i}(3g). \quad (4)$$

The last diagram with the non-abelian ggg vertex has a surprise for the gluon on-shell.

4) Background

• For decades, $\hat{\mu}_t$ has been investigated via dipolar couplings in the context of tree level calculations and experiments on the production of $t\bar{t}$, P. Haberl, O. Nachtmann, and A. Wilch [1].

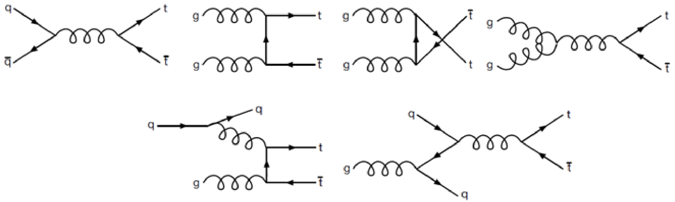

• 2008. R. Martínez, M. A. Pérez-Angón and N. Poveda [2] reported a $\hat{\mu}_t(q^2 = 0)$ finite with the gluon on-shell in the SM at one-loop level. In fact, as we will see, at $q^2 = 0$ it develops an IR divergence.

5) Background

- 2015. Choudhury and Lahiri [3] found $\hat{\mu}_{q_i}(q^2 = 0) \propto \int_0^1 dx(1-x)^2/x$ $= \mathit{IR\ divergent}$, due to the diagram with the ggg vertex. Instead, they proposed to evaluate $\hat{\mu}_{q_i}(q^2 = -m_Z^2)$, at the high energy convention scale of m_Z, just as $\alpha_s(m_Z^2)$ and $s_W(m_Z^2)$. Despite this, in [3] there are algebraic and numerical mistakes even in the triple gluon vertex diagram.

- 2017. A. Bashir, R. Bermúdez, et al. [4], from Davydychev [5] (2001), reported the pure QCD contribution for a small quark case, they also show $\hat{\mu}_{q_i}(q^2 = 0) \propto \ln(-m_{q_i}^2/q^2) = \mathit{IR\ divergent}$.

5) Background: our prediction from the 3-body vertex

- 2018. In [6] we published $\hat{\mu}_t$ in the SM (no analytical details where given there):

$\hat{\mu}_t$	q^2		
	Spacelike $-m_Z^2$	0	Timelike m_Z^2
Total	$-2.24 \times 10^{-2} - 9.25 \times 10^{-4} i$	IR div.	$-1.33 \times 10^{-2} - 2.67 \times 10^{-2} i$

- 2020. The LHC CMS Collaboration [7] reported by the first time an exact measurement of $\hat{\mu}_t$ using pp collisions at the c.m. energy of 13 TeV:

$$\hat{\mu}_t^{\mathrm{Exp}} = -0.024^{+0.013}_{-0.009}(\mathrm{stat})^{+0.016}_{-0.011}(\mathrm{syst}).$$

- 2021. In [8] we published analytical details of $\hat{\mu}_t$, in particular the dimensional regularization (DR) of the Passarino-Veltman scalar function (PaVe) $B_0(q^2, 0, 0)$ of the 3g vertex diagram, that besides its intrinsic UV divergence it develops an IR divergence when $B_0(0, 0, 0)$.
- 2021. A. I. Hernández-Juárez, A. Moyotl and G. Tavares-Velasco in [9] confirmed our results published in [6] and [8].

6) Background: our prediction from the 3-body vertex

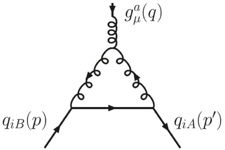

Contribution of the 3-gluon vertex diagram

$$\hat{\mu}_{q_i}(3g) = \frac{3\alpha_s}{4\pi}\frac{m_{q_i}^4}{(q^2-4m_{q_i}^2)^2}\left\{8-\frac{2q^2}{m_{q_i}^2}+\left(8+\frac{q^2}{m_{q_i}^2}\right)\right. \tag{5}$$

$$\left.\times\left[B_0(m_{q_i}^2,0,m_{q_i}^2)-B_0(q^2,0,0)\right]-6q^2C_0(m_{q_i}^2,m_{q_i}^2,q^2,0,m_{q_i}^2,0)\right\},$$

$$B_0(m_q^2,0,m_q^2) = \Delta_{\rm UV}+\ln\frac{\mu^2}{m_q^2}+2, \tag{6}$$

$$B_0(q^2,0,0) = -i16\pi^2\mu^{2\epsilon}\int\frac{d^Dk}{(2\pi)^D}\frac{1}{k^2(k+q)^2} = \Delta_{\rm UV}+\ln\frac{\mu^2}{-q^2}+2, \tag{7}$$

$$\Delta_{\rm UV}\equiv\frac{1}{\epsilon_{\rm UV}}-\gamma_E+\ln 4\pi,\quad \epsilon_{\rm UV}\equiv\epsilon=\frac{4-D}{2}\gtrsim 0. \tag{8}$$

7) Background: our prediction from the 3-body vertex

Then

$$B_0(m_{q_i}^2, 0, m_{q_i}^2) - B_0(q^2, 0, 0) = -\ln \frac{m_{q_i}^2}{-q^2}, \quad \text{for } q^2 \neq 0. \tag{9}$$

By dimensional regularization it can be shown that

$$\begin{aligned} B_0(0,0,0) &= \frac{1}{\epsilon_{\mathrm{UV}}} - \frac{1}{\epsilon_{\mathrm{IR}}} \\ &= \Delta_{\mathrm{UV}} - \Delta_{\mathrm{IR}}, \end{aligned} \tag{10}$$

$$\Delta_{\mathrm{IR}} \equiv \frac{1}{\epsilon_{\mathrm{IR}}} - \gamma_E + \ln 4\pi, \quad \epsilon_{\mathrm{IR}} \equiv \epsilon = \frac{4-D}{2} \lesssim 0. \tag{11}$$

therefore

$$B_0(m_{q_i}^2, 0, m_{q_i}^2) - B_0(0,0,0) = \Delta_{\mathrm{IR}} + \ln \frac{\mu^2}{m_{q_i}^2} + 2, \tag{12}$$

and finally

$$\lim_{q^2 \to 0} \hat{\mu}_{q_i}(3g) = \frac{3\alpha_s}{8\pi} \left(\Delta_{\mathrm{IR}} + \ln \frac{\mu^2}{m_{q_i}^2} + 3 \right). \tag{13}$$

8) Background: our prediction from the 3-body vertex

$$\hat{\mu}_t^{\text{Exp}} = -0.024^{+0.013}_{-0.009}(\text{stat})^{+0.016}_{-0.011}(\text{syst}).$$

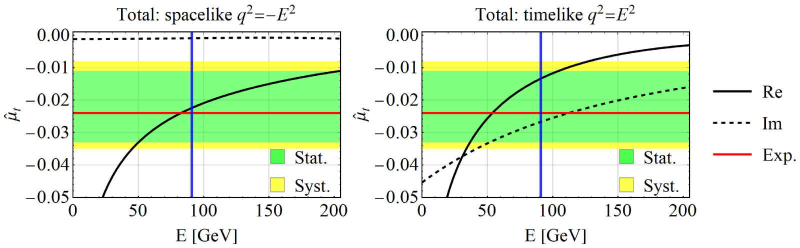

The vertical blue line indicates the energy scale $E = m_Z$.

$$\hat{\mu}_t(-m_Z^2) = -0.0224 - 0.000923i \quad , \quad \hat{\mu}_t(m_Z^2) = -0.0133 - 0.0267i.$$

$$\|\hat{\mu}_t(q^2 = -m_Z^2)\| = 0.0224 \quad , \quad \|\hat{\mu}_t(q^2 = m_Z^2)\| = 0.0298.$$

Our $q^2 = -m_Z^2$ prediction matches with the experiment.

– IS THAT ALL?

– NO, QCD OFFERS MORE!

10) The QCD exclusive 4-body vertex dipolar coupling $gg\bar{q}q$

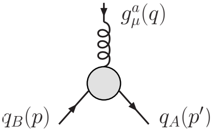

$T^a_{AB}\sigma^{\mu\nu}q_\nu[\mu_q(s) + id_q(s)\gamma^5]$

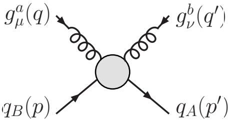

$ig_s f_{abc}T^c_{AB}\sigma^{\mu\nu}[\mu_q(s) + id_q(s)\gamma^5]$

The vertical blue line indicates the energy scale $E = m_Z$.

The Lagrangian predicts that μ and d are proportional to $g\bar{q}q$, but also to $gg\bar{q}q$:

$$\mathcal{L}^{5D}_{eff} = -\frac{1}{2}\bar{q}_A\sigma^{\mu\nu}\left[\mu_q(s) + id_q(s)\gamma^5\right] q_B\, G^a_{\mu\nu}\, T^a_{AB}, \tag{14}$$

$$G^a_{\mu\nu} = \partial_\mu g^a_\nu - \partial_\nu g^a_\mu - g_s f_{abc} g^b_\mu g^c_\nu, \tag{15}$$

10) Dipolar 4-body vertex $gg\bar{q}q$ content in the SM

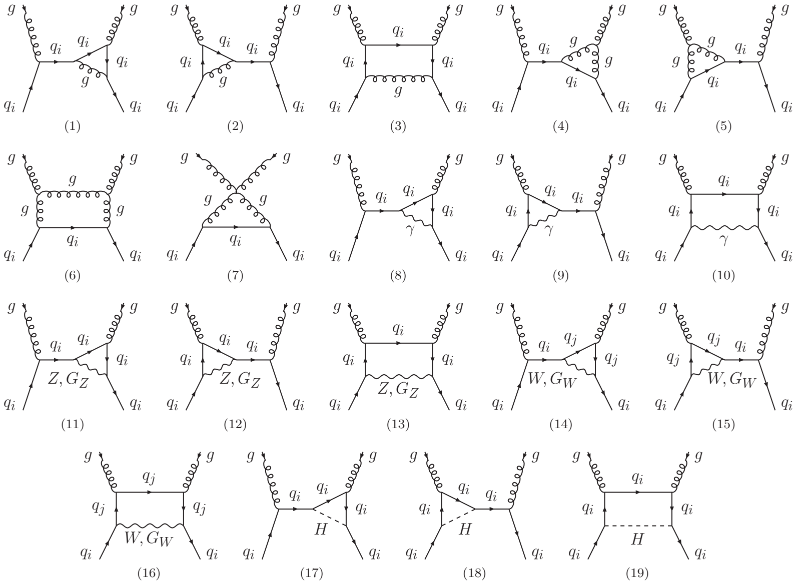

73 diagrams participate in the Feynman-'t Hooft gauge $\xi = 1$.

11) Virtual gluon contribution to $gg\bar{q}q$

$\hat{\mu}_t(g)$ contribution for the Lorentz invariant $s \neq 0$, IR divergent if $s = 0$:

$$
\begin{aligned}
\hat{\mu}_t(g) = \frac{\alpha_s m_t^2}{24\pi(4m_t^2 - s)} \Bigg[& -34 \frac{\left(5m_t^2 - 2s\right)\left(10m_t^4 - 18m_t^2 s + 5s^2\right)}{\left(m_t^2 - s\right)\left(9m_t^4 - 16m_t^2 s + 4s^2\right)} B^g_{0(1)} + 72 B^g_{0(2)} \\
& + 34 \frac{\left(4m_t^2 - s\right)\left(12m_t^4 - 23m_t^2 s + 8s^2\right)}{\left(m_t^2 - s\right)\left(9m_t^4 - 16m_t^2 s + 4s^2\right)} B^g_{0(3)} - 4 B^g_{0(4)} \\
& - 72 \frac{\left(2m_t^2 - 3s\right)\left(4m_t^2 - s\right)}{9m_t^4 - 16m_t^2 s + 4s^2} B^g_{0(5)} + 4 \frac{\left(4m_t^2 - s\right)\left(2m_t^2 - 3s\right)}{9m_t^4 - 16m_t^2 s + 4s^2} B^g_{0(6)} \\
& + 18\left(2m_t^2 - s\right) C^g_{0(1)} - 4\left(m_t^2 - s\right) C^g_{0(2)} + 2\left(m_t^2 - s\right) C^g_{0(3)} \\
& - 9\left(2m_t^2 - s\right) C^g_{0(4)} + 36 s C^g_{0(5)} + 2\left(4m_t^2 - s\right) C^g_{0(6)} \\
& + 9 \frac{14m_t^6 - 79m_t^4 s + 100m_t^2 s^2 - 20s^3}{9m_t^4 - 16m_t^2 s + 4s^2} C^g_{0(7)} \\
& - 2 \frac{31m_t^6 - 61m_t^4 s + 23m_t^2 s^2 - 2s^3}{9m_t^4 - 16m_t^2 s + 4s^2} C^g_{0(8)} + 9s\left(2m_t^2 - s\right) D^g_{0(1)} \\
& + 2\left(m_t^2 - s\right)\left(4m_t^2 - s\right) D^g_{0(2)} \Bigg],
\end{aligned}
\tag{16}
$$

All the Lorentz invariants are considered at the same energy scale s, because in the vertex none of them is privileged over any other, all are equally important: $(q + q')^2 = (p - p')^2 = (q + p)^2 = (p' - q')^2 = (p + q')^2 = (p' - q)^2 \equiv s \neq 0$.

12) Virtual gluon contribution to $gg\bar{q}q$

Passarino-Veltman scalar functions:

$B^g_{0(1)} \equiv B_0(m_t^2; 0, m_t)$,
$B^g_{0(2)} \equiv B_0(s\,; 0, 0)$,
$B^g_{0(3)} \equiv B_0(s\,; 0, m_t)$,
$B^g_{0(4)} \equiv B_0(s\,; m_t, m_t)$,
$B^g_{0(5)} \equiv B_0(-2m_t^2 + 3s\,; 0, 0)$,
$B^g_{0(6)} \equiv B_0(-2m_t^2 + 3s\,; m_t, m_t)$,
$C^g_{0(1)} \equiv C_0(0, s, -2m_t^2 + 3s\,; 0, 0, 0)_{\rm IR}$,
$C^g_{0(2)} \equiv C_0(0, s, -2m_t^2 + 3s\,; m_t, m_t, m_t)$,
$C^g_{0(3)} \equiv C_0(m_t^2, 0, s\,; 0, m_t, m_t)$,
$C^g_{0(4)} \equiv C_0(m_t^2, 0, s\,; m_t, 0, 0)_{\rm IR}$,
$C^g_{0(5)} \equiv C_0(m_t^2, m_t^2, s\,; 0, m_t, 0)$,
$C^g_{0(6)} \equiv C_0(m_t^2, m_t^2, s\,;\ m_t, 0, m_t)_{\rm IR}$,
$C^g_{0(7)} \equiv C_0(m_t^2, s, -2m_t^2 + 3s\,; 0, m_t, 0)$,
$C^g_{0(8)} \equiv C_0(m_t^2, s, -2m_t^2 + 3s\,;\ m_t, 0, m_t)$,
$D^g_{0(1)} \equiv D_0(m_t^2, m_t^2, 0,\ -2m_t^2 + 3s, s, s\,; 0, m_t, 0, 0)_{\rm IR}$,
$D^g_{0(2)} \equiv D_0(m_t^2, m_t^2, 0,\ -2m_t^2 + 3s, s, s\,; m_t, 0, m_t, m_t)_{\rm IR}$.

13) Virtual gluon contribution to $gg\bar{q}q$

Sample of IR Passarino-Veltman scalar functions, even if $s \neq 0$:

$$
\begin{aligned}
C^{g}_{0(4)} &\equiv C_0(m^2_{q_i}, 0, s\,; m_q, 0, 0) \\
&= \frac{-1}{2(m_q^2 - s)} \Bigg[\Delta_{\rm IR2} + \Delta_{\rm IR} \left(\ln \frac{\mu^2}{m_q^2} + 2\ln \frac{m_q^2}{m_q^2 - s} \right) + 2\ln \frac{\mu^2}{m_q^2} \ln \frac{m_q^2}{m_q^2 - s} \\
&+ \frac{1}{2} \ln^2 \frac{\mu^2}{m_q^2} - 2\mathrm{Li}_2 \frac{s}{s - m_q^2} + \ln^2 \frac{m_q^2}{m_q^2 - s} + \frac{\pi^2}{12} \Bigg],
\end{aligned}
\tag{17}
$$

$$
\begin{aligned}
D^{g}_{0(2)} &\equiv D_0(m_q^2, m_q^2, 0, -2m_q^2 + 3s, s, s\,; m_q, 0, m_q, m_q) \\
&= \frac{1}{(m_q^2 - s)\,(4m_q^2 - s)} \left(\Delta_{\rm IR} + \ln \frac{\mu^2}{m_q^2} \right) \frac{R_1}{s} \ln \frac{2m_q^2 - s + R_1}{2m_q^2} \\
&+ \frac{2}{(m_q^2 - s)\,R_1} \Bigg[\frac{R_1}{4m_q^2 - s} \left(\ln \frac{m_q^2}{m_q^2 - s} - \ln \frac{4sR_1}{(s + R_1)^2} \right) \frac{R_1}{s} \ln \frac{2m_q^2 - s + R_1}{2m_q^2} \\
&+ \frac{1}{2} \ln^2 \frac{4m_q^2 - 3s + R_2}{2m_q^2} + \frac{1}{2} \mathrm{Li}_2 \left(\frac{s - R_1}{s + R_1} \right)^2 - \frac{\pi^2}{12} \\
&+ \mathcal{L}i_2 \left(\frac{R_1 - s}{R_1 + s} - i\varepsilon, \frac{4m_q^2 - 3s + R_2}{2m_q^2} + \frac{R_2}{m_q^2} i\varepsilon \right) \\
&+ \mathcal{L}i_2 \left(\frac{R_1 - s}{R_1 + s} - i\varepsilon, \frac{4m_q^2 - 3s - R_2}{2m_q^2} - \frac{R_2}{m_q^2} i\varepsilon \right) \Bigg],
\end{aligned}
\tag{18}
$$

14) Virtual gluon contribution to $gg\bar{q}q$

where $R_1 \equiv \sqrt{s(s-4m_q^2)}$, $R_2 \equiv \sqrt{3(2m_q^2-3s)(2m_q^2-s)}$, $\mathcal{L}i_2$ is the Beenakker-Denner continued dilogarithm and the IR poles are

$$\Delta_{\mathrm{IR}} \equiv \frac{1}{\epsilon_{\mathrm{IR}}} - \gamma_E + \ln 4\pi, \tag{19}$$

$$\Delta_{\mathrm{IR2}} \equiv \frac{1}{\epsilon_{\mathrm{IR}}^2} + \frac{1}{\epsilon_{\mathrm{IR}}}(-\gamma_E + \ln 4\pi) + \frac{\gamma_E^2}{2} - \gamma_E \ln 4\pi + \frac{1}{2}\ln^2 4\pi + \frac{\pi^2}{12}. \tag{20}$$

- $\hat{\mu}_t(g)$ is IR finite for $s \neq 0$, only IR divergent when $s = 0$.
- $\hat{\mu}_t(\gamma)$ is IR finite for $s \neq 0$ and $s = 0$, despite it has some IR PaVes.
- $\hat{\mu}_t(Z)$, $\hat{\mu}_t(W)$ and $\hat{\mu}_t(H)$ have no IR PaVes.
- The CEDM $\hat{d}_t = 0$

15) $\hat{\mu}_t^{3b}$ vs. $\hat{\mu}_t^{4b}$ in the SM

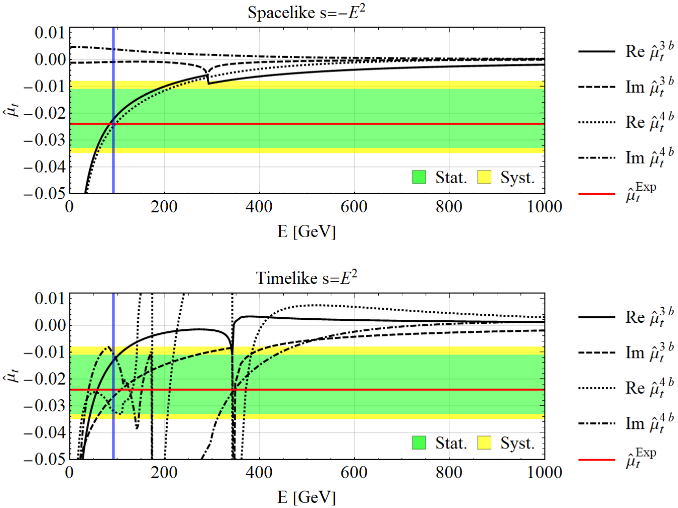

- Only the spacelike evaluation is well behaved.
- In the spacelike evaluation the Im part is due to the W contribution.

15) $\hat{\mu}_t^{3\mathrm{b}}$ vs. $\hat{\mu}_t^{4\mathrm{b}}$ in the SM

$$\hat{\mu}_t^{\mathrm{Exp}} = -0.024^{+0.013}_{-0.009}(\mathrm{stat})^{+0.016}_{-0.011}(\mathrm{syst}).$$

Contribution	$\hat{\mu}_t(-m_Z^2)$	
	3-body	4-body
g	-2.27×10^{-2}	-2.54×10^{-2}
γ	2.62×10^{-4}	-5.19×10^{-4}
Z	-1.76×10^{-3}	-1.78×10^{-3}
W	$-2.89 \times 10^{-5} - 9.23 \times 10^{-4} i$	$-3.43 \times 10^{-4} + 3.84 \times 10^{-3} i$
H	1.85×10^{-3}	3.06×10^{-3}
Total	$-2.24 \times 10^{-2} - 9.23 \times 10^{-4} i$	$-2.5 \times 10^{-2} + 3.84 \times 10^{-3} i$

Spacelike

Contribution	$\hat{\mu}_t(m_Z^2)$	
	3-body	4-body
g	$-1.38 \times 10^{-2} - 2.55 \times 10^{-2} i$	$-2.62 \times 10^{-2} - 1.44 \times 10^{-2} i$
γ	2.88×10^{-4}	-6.76×10^{-4}
Z	-1.88×10^{-3}	-1.85×10^{-3}
W	$1.41 \times 10^{-4} - 1.16 \times 10^{-3} i$	$-6.24 \times 10^{-3} + 3.78 \times 10^{-3} i$
H	1.98×10^{-3}	3.19×10^{-3}
Total	$-1.33 \times 10^{-2} - 2.67 \times 10^{-2} i$	$-3.18 \times 10^{-2} - 1.06 \times 10^{-2} i$

Timelike

16) $\hat{\mu}_t^{\rm 3b}$ vs. $\hat{\mu}_t^{\rm 4b}$ in the SM

$$\hat{\mu}_t^{\rm Exp} = -0.024^{+0.013}_{-0.009}({\rm stat})^{+0.016}_{-0.011}({\rm syst}).$$

The spacelike values corner $\|\hat{\mu}_t^{\rm Exp}\|$:

$$\|\hat{\mu}_t^{\rm 3b}(-m_Z^2)\| \lessapprox \|\hat{\mu}_t^{\rm EXP}\| \lessapprox \|\hat{\mu}_t^{\rm 4b}(-m_Z^2)\|,$$

$$0.0224 \lessapprox 0.0240 \lessapprox 0.0253,$$

The timelike values move away from $\|\hat{\mu}_t^{\rm Exp}\|$:

$$\|\hat{\mu}_t(m_Z^2)^{\rm 3b}\| = 0.0298 \qquad , \quad \|\hat{\mu}_t(m_Z^2)^{\rm 4b}\| = 0.0335.$$

20) Conclusions

• We have derived $\hat{\mu}_t$ from the 3- and 4-body vertex functions as predicted by the Lagrangian, the calculation has been made in a process independent way.

• $\hat{\mu}_t^{\rm 3b}(s)$ and $\hat{\mu}_t^{\rm 4b}(s)$ are IR divergent at $s = 0$.

• The spacelike evaluation, $s = -E^2$, is the well-behaved one. The imaginary part is induced by the W contribution.

• Theoretically is expected $\hat{\mu}_t^{\rm 3b}{=}\hat{\mu}_t^{\rm 4b}$, nevertheless, our numerical evaluations show that $\mathrm{Re}\,\hat{\mu}_t^{\rm 3b} \approx \mathrm{Re}\,\hat{\mu}_t^{\rm 4b}$.

• The evaluation of $\hat{\mu}_t^{\rm 3b}(s)$ and $\hat{\mu}_t^{\rm 4b}(s)$ at the energy scale of $s = -m_Z^2$, as $\alpha_s(m_Z^2)$ and $s_W(m_Z^2)$ are conventionally evaluated, encloses the experimental value: $\|\hat{\mu}_t^{\rm 3b}(-m_Z^2)\| \lessapprox \|\hat{\mu}_t^{\rm EXP}\| \lessapprox \|\hat{\mu}_t^{\rm 4b}(-m_Z^2)\|$.

References

[1] P. Haberl, O. Nachtmann and A. Wilch, "Top production in hadron hadron collisions and anomalous top-gluon couplings," Phys. Rev. D **53**, 4875 (1996) doi:10.1103/PhysRevD.53.4875 [hep-ph/9505409].

[2] R. Martínez, M. A. Pérez and N. Poveda, "Chromomagnetic Dipole Moment of the Top Quark Revisited," Eur. Phys. J. C **53**, 221 (2008) doi:10.1140/epjc/s10052-007-0457-6 [hep-ph/0701098].

[3] I. D. Choudhury and A. Lahiri, "Anomalous chromomagnetic moment of quarks," Mod. Phys. Lett. A **30**, no. 23, 1550113 (2015) doi:10.1142/S0217732315501138 [arXiv:1409.0073 [hep-ph]].

[4] R. Bermudez, L. Albino, L. X. Gutiérrez-Guerrero, M. E. Tejeda-Yeomans and A. Bashir, "Quark-gluon Vertex: A Perturbation Theory Primer and Beyond," Phys. Rev. D **95**, no. 3, 034041 (2017) doi:10.1103/PhysRevD.95.034041 [arXiv:1702.04437 [hep-ph]].

[5] A. I. Davydychev, P. Osland and L. Saks, "Quark gluon vertex in arbitrary gauge and dimension," Phys. Rev. D **63**, 014022 (2001) doi:10.1103/PhysRevD.63.014022 [hep-ph/0008171].

[6] J. I. Aranda, D. Espinosa-Gómez, J. Montaño, B. Quezadas-Vivian, F. Ramírez-Zavaleta and E. S. Tututi, "Flavor violation in chromo- and electromagnetic dipole moments induced by Z' gauge bosons and a brief revisit of the Standard Model," Phys. Rev. D **98**, no. 11, 116003 (2018) doi:10.1103/PhysRevD.98.116003 [arXiv:1809.02817 [hep-ph]].

[7] A. M. Sirunyan *et al.* [CMS], "Measurement of the top quark forward-backward production asymmetry and the anomalous chromoelectric and chromomagnetic moments in pp collisions at $\sqrt{s} = 13$ TeV," JHEP **06**, 146 (2020) doi:10.1007/JHEP06(2020)146 [arXiv:1912.09540 [hep-ex]].

[8] J. I. Aranda, T. Cisneros-Pérez, J. Montaño, B. Quezadas-Vivian, F. Ramírez-Zavaleta and E. S. Tututi, "Revisiting the top quark chromomagnetic dipole moment in the SM," Eur. Phys. J. Plus **136**, no.2, 164 (2021) doi:10.1140/epjp/s13360-021-01102-x [arXiv:2009.05195 [hep-ph]].

[9] A. I. Hernández-Juárez, A. Moyotl and G. Tavares-Velasco, "New estimate of the chromomagnetic dipole moment of quarks in the standard model," Eur. Phys. J. Plus **136**, no.2, 262 (2021) doi:10.1140/epjp/s13360-021-01239-9 [arXiv:2009.11955 [hep-ph]].